

Investigation of Sintering Processes by Tomography

B. Kieback^{1, a}, M. Nöthe^{1, b}, J. Banhart^{2, c}, R. Grupp^{1,2, d}

¹ Technische Universität Dresden, Institute of Materials Science, 01062 Dresden, Germany

² Helmholtz Centre Berlin for Materials and Energy, Berlin, Germany

^a bernd.kieback@ifam-dd.fraunhofer.de, ^b michael.noethe@tu-dresden.de,

^c banhart@helmholtz-berlin.de, ^d rainer.grupp@helmholtz-berlin.de

Keywords: sintering, fundamentals, tomography

Abstract

Sintering especially of loose particle packings is accompanied by dimensional changes of the specimen. The growth of inter particle contacts under the influence of the Laplace pressure is well understood and described by the two particle model. On the other hand the understanding of other fundamental sintering phenomena i.e. cooperative material transport processes is rather vague. To overcome this limitation for near net-shape production of components by powder metallurgy an improved model of particle rearrangement processes is required. First efforts to obtain necessary experimental data were performed at 1D and 2D models. But recent improvements of high resolution synchrotron computer tomography (SCT) setups allow the acquisition of in-situ data of particle rearrangements.

In-situ studies of particle rotations during sintering were conducted at the ESRF in Grenoble. The rotations during free sintering of monocrystalline particles were investigated during continuous heating up to 1050 °C or with frequent interruptions of the heating by 1 hr dwell times every 100 °C. In contrast to 1D specimens measured by Wieters the 3D specimens showed negligible rotations. This must be attributed to the constraints in 3D samples. To obtain a more detailed insight in the rotations the particles of one sample were marked. It is possible to show that the particles perform intrinsic rotations. Therefore a new rotation model is developed. The intrinsic rotations are confirmed by complementary EBSD analyses as well.

Introduction

Sintering of assemblies of loose or compacted particles is the most important processing step during the production of powder metallurgical components. This heat treatment results in the shrinkage of the component and a growth of interparticle bonds. The growth of sintering necks driven by the Laplace pressure is described by the well known two particle model. Excellent reviews were published by J.E. Geguzin [1], H.E. Exner [2, 3], W. Schatt [4] and R.M. German [5].

In sintering specimens additional, cooperative material transport processes (movements of particles) occur and contribute to discrepancies between the calculated and measured densifications. Major driving forces for rotations are asymmetric sintering necks [4], non uniform sintering activity [6] and the need to form low energy contact grain boundaries [7]. To achieve a fundamental understanding of these processes the employment of new analysis technologies is essential. High resolution tomography combined with photogrammetric image analyzing is the best method to obtain the required experimental data base. First investigations of sintering processes by synchrotron computed tomography (SCT) have been made by Vagnon et. al. [8] and O. Lame et. al. [9]. Micro focus computed tomography combined with photogrammetric image analyzing was used by Nöthe et. al. [10]. In this context SCT allows the combination of in-situ measurements and enhanced accuracy of image analysis due to the excellent image quality.

Experimental

Spherical copper powders were used. The raw material was air atomized copper provided by the company ECKA Granulate GmbH & Co. KG. The monocrystalline copper particles were produced by the Sauerwald process [11]. Rolling the particles down a tilted glass panel was used to select ideally spherical particles. To observe intrinsic rotations of particles some of the specimens consisted of spheres marked with small (about $8 \times 8 \times 12 \mu\text{m}$) holes drilled by a focused ion beam (FIB).

The copper powder was filled into silica capillaries ($\text{Ø } 1.3\text{mm}$) and fixed in a pre-sintering step at $600 \text{ }^\circ\text{C}$. After the pre-sintering step the capillary could be removed to analyze free sintering. The first specimen consisting of marked particles was not pre-sintered to enable the measurement of intrinsic rotations at low temperatures. The drawback was that the sintering of this specimen was constrained.

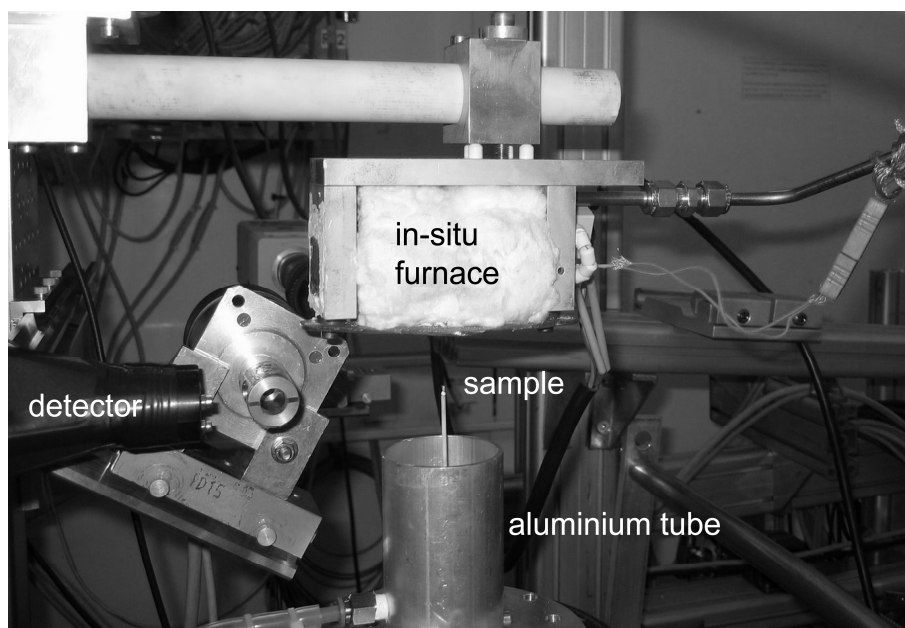


Fig. 1 Tomography setup at ESRF. The furnace is lifted to change the sample. In operation a continuous N_2 -flow in the Al tube seals the furnace atmosphere.

The in-situ measurements were conducted at the European Synchrotron Radiation Facility (ESRF) in Grenoble at the beamline ID 15 A. The in-situ furnace (Fig. 1) provided by the ESRF operated with a reducing atmosphere ($96\% \text{He} + 4\% \text{H}_2$). The beamline allows the use of a white beam. This way the necessary 851 radiograms per high quality tomogram could be acquired within 85 seconds. Including the acquisition of 51 flatfield radiograms, the sample movements and camera readout the entire measurement of one tomogram took 212 seconds. These fast measurements enabled the analysis of the specimen during the continuous sintering process. The specimens were heated with a rate of 10 K/min and the heating was interrupted for one hour dwell times at $650 \text{ }^\circ\text{C}$, $750 \text{ }^\circ\text{C}$, $850 \text{ }^\circ\text{C}$, $950 \text{ }^\circ\text{C}$ and $1050 \text{ }^\circ\text{C}$.

To obtain quantitative data special image analysis software was developed [12]. The particles are identified by searching spherical regions exceeding a grey value threshold. The approximate particle centres identified in the first step are refined in a subsequent step. The accurate position of the particle surface is determined by analyzing the grey value lines originating in the preliminary particle centre. A sphere function is fitted through the surface points. In addition to the accurate particle positions the software is able to track all particles over the entire sintering process and to identify the coordination partners of the particles.

Based on these image-analysis results the particle centre approach, the local density and the shrinkage of the specimen can be computed. The rolling with respect to the coordination partners is

determined by fitting the particle and its coordination partners to their positions in a different sintering step and calculating the angle changes between the particle and its coordination partners. The error of the calculated rotation is about 0.1° .

Results and discussion

Fig. 2 shows both the cumulative rotation and the particle centre approach during the sintering of samples consisting of single crystalline copper spheres of $60\ \mu\text{m}$ diameter. The thermal expansion was subtracted. Below 950°C the sample shows a slight increase of the distance between the particle centres. During the dwell time at 950°C the specimen shows an additional centre approach compared with a specimen without dwell time. At higher temperature the specimen shows a particle centre approach with a steep increase at 1050°C .

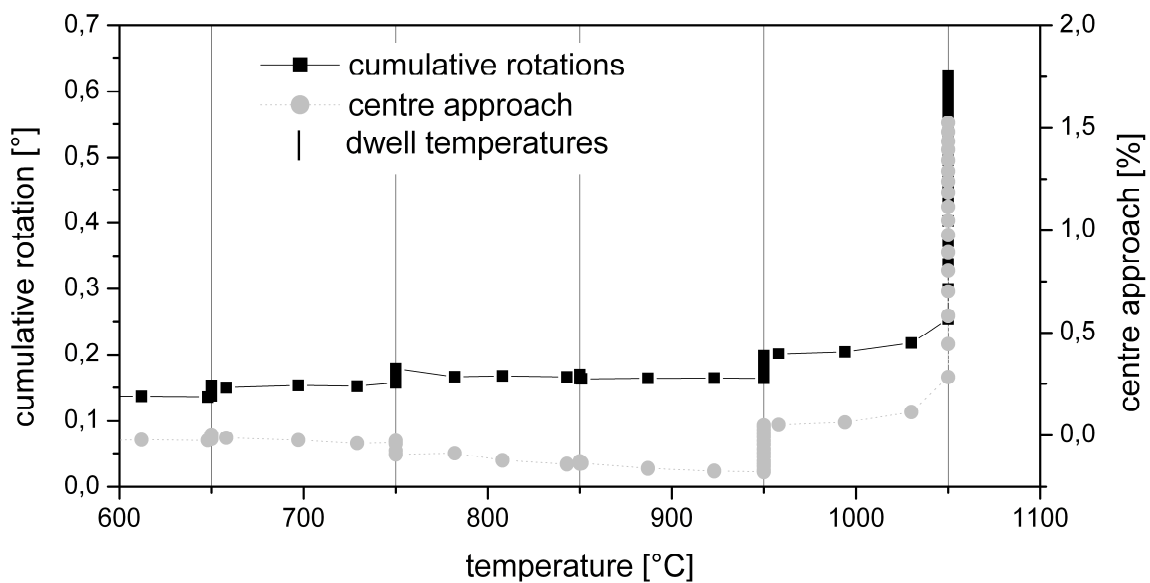


Fig. 2 Cumulative rotation and centre approach vs. temperature of monocrystalline copper specimens. Particle diameters approx. $60\ \mu\text{m}$. Heating rate $10\ \text{K/min}$. Dwell times $60\ \text{min}$.

Below 950°C insignificant rotations take place. Nevertheless the slight expansion of the particle centre distance must be attributed to those small rotations. At 950°C the specimen with dwell time shows a slightly increased rotation. In both specimens the obvious rotations occur at temperatures of 1050°C and peak to 0.7° (after 1 hour of dwell time at 1050°C). These values are minute compared to the 25° rotations of rows of copper spheres reported by K.-P. Wieters [13] and sphere plate experiments [14]. The extensive rotations reported in literature occurred at temperatures between 600°C and 900°C [13]. In these early stages of sintering the contact areas are minute and the models offered a high degree of freedom to accommodate the driving forces. Thus fast rotations driven by the need to form low energy grain boundaries can occur. The small rotations observed by SCT are explained easily. The particles have (see Fig. 4) 6 to 7 contact partners. The superimposed driving forces of the various contacts hamper the rotation. Significant rotations due to inhomogeneous particle centre approach can only occur at high temperatures, indicated by the increase of the graphs in Fig. 2. As both the extensive rotations and the extensive particle centre approach occur at the same temperature it can be concluded, that the inhomogeneous centre approach is the dominant driving force of the observed rotations.

Fig. 3 shows the distributions of cumulative rotation for 5 sintering stages. As already shown the average cumulative rotation increases with progress of the sintering process. All distributions have the shape of a Gauss function. This proves that the continuous increase of the average rotation is

caused by continuous rotations of all particles and not by singular particles performing extensive rotations.

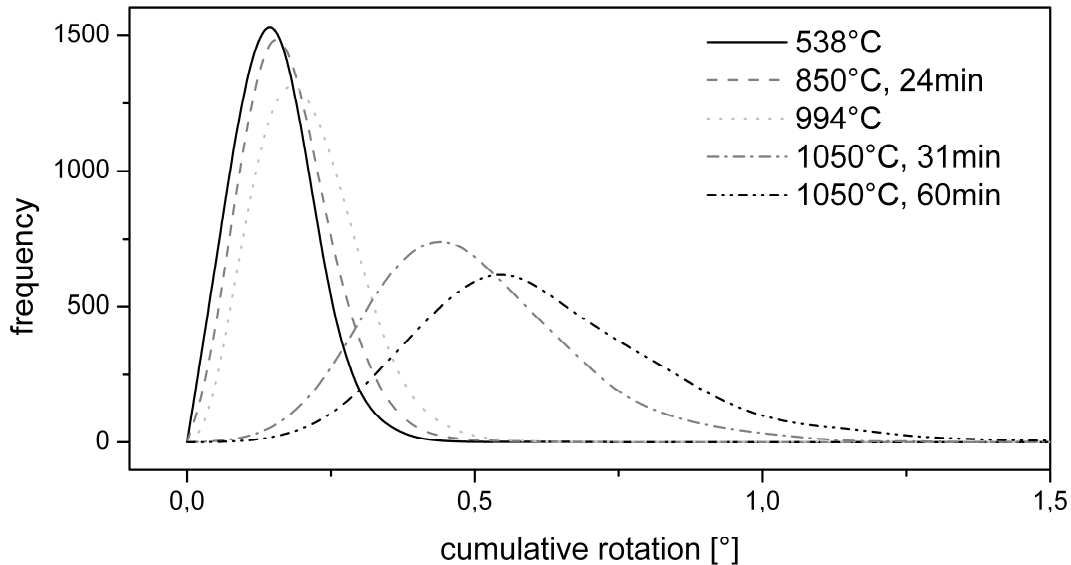


Figure 3 Histogram of the cumulative rotations in various sintering stages. Particle diameters approx. 60 μm . Heating rate 10 K/min. Dwell times 60 min.

Fig. 4 shows average coordination plotted vs. the temperature. The specimen shows an increase of the coordination at the beginning of each dwell time and a decrease of coordination at the beginning of each heating step below 950 $^{\circ}\text{C}$. Obviously the minute rotations at low temperatures have an unexpectedly clear influence on the sintering process during heating periods.

First results of preliminary experiments using marked spheres as well as EBSD analyses of sintering rows on copper plates show that extensive intrinsic rotations occur during sintering.

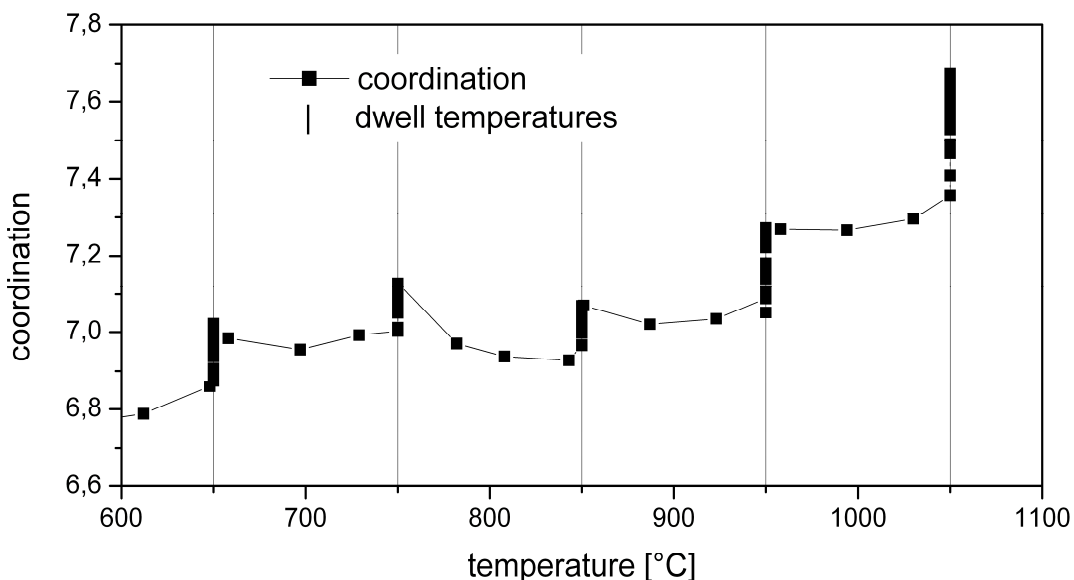


Figure 4 Average coordination vs. temperature of monocrystalline copper powder. Particle diameters approx. 60 μm . Heating rate 10 K/min. Dwell times 60 min.

Fig. 5 shows the coordination of the particles plotted vs. the density compared to various values found in literature. The coordination numbers match the literature values very well. This proves that

SCT combined with photogrammetric image analyzing can provide a highly accurate analysis of particle coordination.

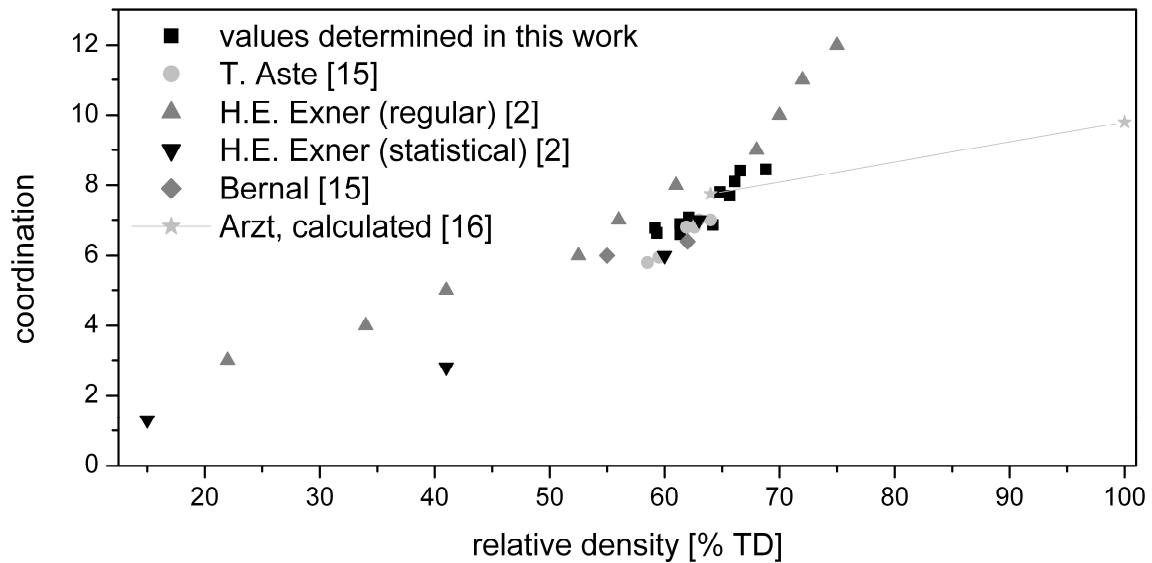


Figure 5 Coordination vs. density. Values determined in this work: multiple samples with monomodal particle sizes with mean values between 40 μm and 100 μm

Conclusion

High resolution synchrotron tomography is an essential tool for the quantitative analysis of cooperative material transport processes.

The behaviour of 3D samples significantly deviates from the behaviour of 1D samples. The explanation of the difference is easy. In 3D samples the superposition of multiple driving forces results in a lower driving force per contact. This and the necessary displacement of neighbouring particles during rotation degrade the rotation activity.

Preliminary experiments show, that intrinsic rotations are very important. The observation of these intrinsic rotations requires a more sophisticated experimental approach using marked particles. The application of markers allows the observation of intrinsic rotations and results of our measurements will be published soon.

Acknowledgements

The authors would like to thank the Helmholtz-Gemeinschaft for the financial support of the research in the project Virtual Institute – Photon and Neutron Research on Advanced Engineering Materials. We would like to thank M. Di Michiel for the support at the ESRF. Furthermore, we are grateful to ECKA Granulate GmbH & Co. KG for the supply of the polycrystalline copper powder.

References

- [1] .E. Geguzin, Physik des Sinterns, VEB Deutscher Verlag für Grundstoffindustrie, Leipzig (1973).
- [2] H.E. Exner, Grundlagen von Sintervorgängen. Berlin/Stuttgart: Gebrüder Borntraeger (1978).
- [3] H.E. Exner, T. Kraft, Review on Computer Simulations of Sintering Processes. *Proc. PM World Congress, Granada*, 278-82 (1998).
- [4] W. Schatt, Sintervorgänge, VDI-Verlag (1992).
- [5] R.M. German., Powder Metallurgy Science, Metal Powder Industries Federation, Princeton (1984).

-
- [6] P.C. Eloff, F.V. Lenel, The Effects of Mechanical Constrains upon the Early Stages of Sintering, *Modern Developments in Powder Metallurgy*, **4**, 291-302 (1971).
- [7] A.P. Sutton, R.W. Balluffi, Interfaces in crystalline materials, Oxford University press (2003).
- [8] A. Vagnon, J.P. Rivière, J.M. Missiaen, D. Bellet, M. Di Michiel, C. Josserond, D. Bouvard, 3D statistical analysis of a copper powder sintering observed in situ by synchrotron microtomography, *Acta Materialia*, **58**, 1084-93 (2008).
- [9] O. Lame, D. Bellet, M. Di Michiel, D. Bouvard, Bulk observation of metal powder sintering by X-ray synchrotron microtomography; *Acta Materialia*, **52**, 977-84 (2004).
- [10] M. Nöthe, M. Schulze, R. Grupp, B. Kieback, A. Haibel, Investigation of sintering of spherical copper powder by micro focus computed tomography (μ CT) and synchrotron tomography, *Materials Science Forum*, **539-543**, 2657-62 (2007).
- [11] F. Sauerwald, L. Holub, Kristallisation zwischen möglichst weitgehend im Strukturgleichgewicht befindlichen Oberflächen; *Zeitschrift für Elektrochemie und angewandte physikalische Chemie*, **39**, 750-53 (1933).
- [12] R. Grupp, Thesis, TU Dresden, in submitted.
- [13] K.P. Wieters, Korngrenzeneinfluß beim defektaktivierten Festphasensintern, Thesis, TU Dresden (1988).
- [14] S.-W. Chan, R.W. Balluffi, Study of Energy vs. Misorientation for Grain Boundaries in Gold by Crystallite Rotation Method – I. [001] Twist Boundaries, *Acta Metallurgica*, **33**, 1113-19 (1985)
- [15] T. Aste, M. Saadatfar, T.J. Senden; Geometrical structure of disordered sphere packings; *Physical Review E*; Vol. 71; 2005; Seite 061302-1 - 061302-15
- [16] E. Arzt; The Influence of an Increasing Particle Coordination on the Densification of Spherical Powders; *Acta Metallurgica*; Vol. 30; 1982; Seite 1883 - 1890